Water Science & Technology

Water Science & Technology Vol 88 No 11, 3009 doi: 10.2166/wst.2023.379

Preparation of emulsion hydrogels encapsulating extractant by the Pickering emulsion template method to recover lanthanum ions in aqueous solutions

Yong Guo, Jindian Cai, Yaodong Liang and Yongjun He *

Department of Chemistry and Chemical Engineering, Xi'an University of Science and Technology, 58 Yanta Middle Road, Beilin District, Xi'an, China
*Corresponding author. E-mail: yongjunhe@xust.edu.cn

YH, 0000-0001-8963-8438

ABSTRACT

To solve the problem of liquid–liquid extraction of La(III), the oil-in-water Pickering emulsions were prepared by utilizing the aqueous solution of sodium alginate as the continuous phase, kerosene-diluted extractant di-(2-ethylhexyl) phosphate (P204) as the dispersed phase, and modified silica as an emulsifier. Then the emulsions were added to a calcium chloride solution to prepare the Pickering emulsion hydrogels (PEHGs) to better remove La(III). The PEHGs were characterized using Fourier transform infrared, thermogravimetric analysis, and scanning electron microscopy. The adsorption properties of PEHGs for La(III) in the aqueous solution were investigated using a UV–vis spectrophotometer. The study found that P204 was successfully coated by hydrogels and reached the highest adsorption capacity of 48 mg/g at pH 4. The amount of adsorption increased with the rise in temperature from 298 to 318 K. La(III) adsorption experimental data were more consistent with the pseudo-second-order kinetic model and the Langmuir isotherm model. Thermodynamic parameters showed that the adsorption of La(III) by PEHGs was a spontaneous endothermic process. The internal diffusion model revealed a linear relationship, indicating that internal diffusion played a role in the adsorption process. The encapsulating property of PEHGs indicated its potential usefulness in industrial wastewater for treating La(III).

Key words: adsorption, di-(2-ethylhexyl) phosphate, lanthanum, Pickering emulsion hydrogels, sodium alginate

HIGHLIGHTS

- Sodium alginate Pickering emulsion gels (PEHGs) were prepared by modified silica-stabilized Pickering emulsions.
- PEHGs coated with P204 showed a high adsorption capacity of 48 mg/g for La(III) at pH 4.
- After five adsorption and desorption experiments of PEHGs, its adsorption capacity was not less than 85% of the initial adsorption capacity.

GRAPHICAL ABSTRACT

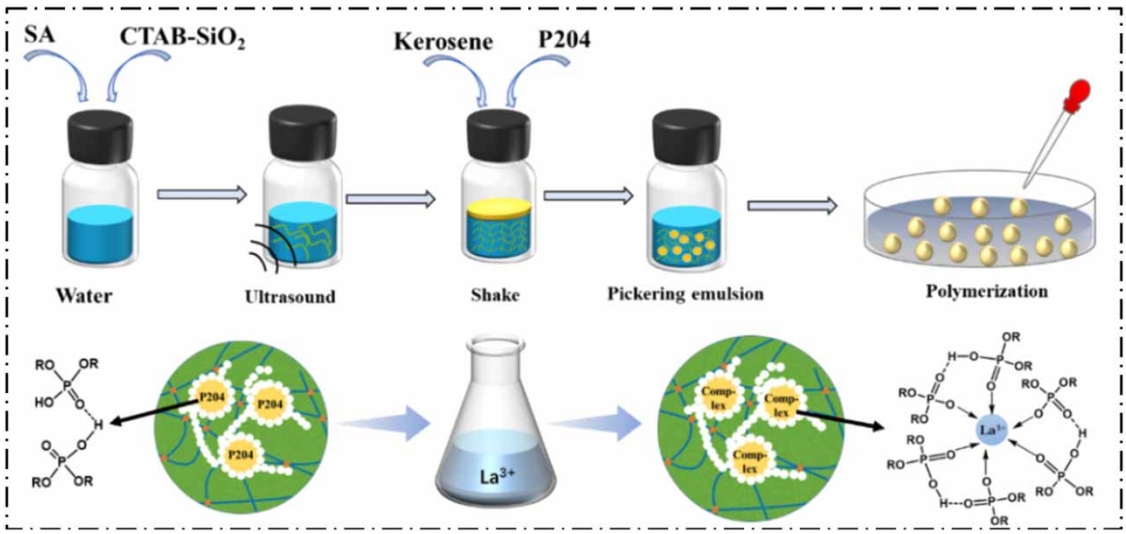

1. INTRODUCTION

Lanthanides possess distinctive physical and chemical properties that have extensive applications in fields such as new energy, new materials, energy conservation, environmental protection, aerospace, and electronic information (Zhou *et al.* 2017). La(III), as a representative of lanthanide elements, is now regarded as a novel contaminant. La(III) is a fission product that may cause harm if released into the environment. La(III) recovery and extraction have consequently attracted a lot of attention.

Now, lanthanides were extracted from an aqueous solution using a variety of techniques, including liquid–liquid extraction (LLE), ion exchange and adsorption, chemical precipitation, membrane extraction separation, and others. Solvent extraction, also known as LLE, was one of the most common methods used in industry to separate and refine lanthanides. This method was mainly through the use of di-(2-ethylhexyl) phosphate (P204), 2-ethylhexyl phosphonic acid mono-2-ethylhexyl ester (P507), and bis-(2,4,4-trimethylpentyl)-phosphinic acid (Cyanex272) extractant to achieve lanthanide recovery and separation (Panda *et al.* 2016; Zhang *et al.* 2021; Xu *et al.* 2022). Even though LLE was frequently employed in industry, the formation of the third phase and the limited contact area between the two phases make it less efficient in extracting rare earth elements. As a result, a lot of research has been done on solid–liquid extraction (SLE) recently (Kumar *et al.* 2010; Ngomsik *et al.* 2012; Radhika *et al.* 2012; Huang *et al.* 2017). SLE offers several advantages, including reducing surfactants and organic extractants, improving contact between extractants and lanthanides in the aqueous phase, and preventing the third equivalent formation and the ability to recover solids for multiple cycles. Therefore, SLE is highly efficient for extracting La(III). The solvent-impregnated resin is the SLE technique that is most frequently employed, and it works by impregnating the best extractant onto selected materials like silica and resin to speed up extraction (Xiaoqi *et al.* 2009; Neagu *et al.* 2010; Lili & Ji 2011). For instance, Mohammedi *et al.* found that the extraction order for Cyanex272 impregnated in porous silica was light lanthanides (La), medium lanthanides (Eu), and then heavy lanthanides (Lu) (Mohammedi *et al.* 2019). El-Sofany prepared impregnated resin that was utilized to extract lanthanum (III) and gadolinium (III) from nitrate media by loading Aliquat-336 onto Amberlite XAD-4 crosslinked polystyrene resin. According to the study, impregnating resin with lanthanum (III) and gadolinium (III) was an efficient way to accomplish so. Additionally, lanthanum (III) and gadolinium (III) had respective adsorption capabilities of 4.73 and 4.44 mg/g (El-Sofany 2008). However, due to the presence of hydrophobic groups, the adsorption efficiency of the impregnated resin prepared by physical impregnation of the extractant into the resin is reduced.

Hydrogel is a three-dimensional network structure polymer material containing a large amount of water (Ahmed 2015), which can provide channels for the diffusion of metal ions (Kobayashi *et al.* 2010; Puguan *et al.* 2015). Therefore, the emulsifying hydrogels that extractants were enveloped in hydrogels have received a lot of interest (Zhang *et al.* 2011; Tokuyama *et al.* 2018). Since conventional emulsions stabilized by surfactants are thermodynamically unstable, it is necessary to find a

way to improve the stability of emulsions. Ramsden and Pickering demonstrated over a century ago that colloidal particles can stabilize emulsions, and such emulsions are called Pickering emulsions (Ramsden 1904). Pickering emulsions have the advantages of cheap cost, minimal emulsifier usage, environmental friendliness, and good emulsion stability over typical surfactant-stabilized emulsions. Therefore, Pickering emulsions can better wrap the extractant. Previous research has shown that Pickering emulsion hydrogels (PEHGs) adsorbed metal cations effectively in aqueous solutions, such as Cu(II), Zn(II), and In(III) (Yuan *et al.* 2021; Dong *et al.* 2023; Gao *et al.* 2023). This technique is generally applicable to other metal ions.

Most colloidal nanoparticles can stabilize Pickering emulsions, and silica nanoparticles are frequently utilized in the stabilization of Pickering emulsions because they are simple to manufacture and manipulate. However, Binks & Lumsdon found that emulsions prepared stabilized by either very hydrophilic or very hydrophobic particles are large and unstable to coalescence (Binks & Lumsdon 2000), because particles are too lipophilic or too hydrophilic and tend to disperse in the oil or aqueous phases, respectively. Binks *et al.* then studied in detail the behavior of a stable dodecane–water emulsion consisting of a mixture of silica nanoparticles and cationic surfactants. Studies have shown that cationic surfactants and nanoparticles can be able to maintain the emulsion, while hydrophilic nanoparticles cannot (Binks *et al.* 2007). Therefore, PEHGs prepared by cationic surfactant-modified silica-stabilized emulsions have high encapsulation efficiency for extractants and have broad application prospects in the recovery of lanthanides in water. However, there are no related reports on this method's recovery of La(III).

In this study, nano-silica (SiO_2) treated with hexadecyl trimethyl ammonium bromide (CTAB) was employed to improve the stability of SiO_2 at the oil–water interface. The oil-in-water (O/W) Pickering emulsions were then stabilized using the modified silica to produce the PEHGs that contain the P204. The encapsulation ability of PEHGs was tested, and they were then used to extract lanthanum ions from the solution. PEHGs were assessed using thermogravimetric (TG) analysis, scanning electron microscopy (SEM), and Fourier transform infrared (FTIR). The impact of temperature, pH level, extractant concentration, and oscillation length on La(III) extraction was then studied. PEHG's ability to adsorb La(III) was studied in terms of thermodynamics and kinetics. The objective of this study was to develop a functional material that efficiently extracts La(III) from industrial wastewater while being economical and environmentally benign.

2. EXPERIMENT

2.1. Experimental materials

All used reagents in the present study are analytical grade and used without any additional purification. Sodium alginate (SA) and calcium chloride ($CaCl_2$) were purchased from Aladdin. Sulfonated kerosene and di-(2-ethylhexyl) phosphate (D2EHPA, P204 $C_{16}H_{35}O_4P$) were purchased from Zhengzhou Hecheng New Materials. Hydrophilic nano-SiO_2 was purchased from Wacker Company. Arsenazo III ($C_{22}H_{18}O_{14}N_4S_2As_2$), glacial acetic acid ($C_2H_4O_2$), sodium acetate ($C_2H_3O_2Na$), nitric acid ($HNO_3$), sodium hydroxide (NaOH), and hexadecyl trimethyl ammonium bromide (CTAB, $C_{19}H_{42}BrN$) were purchased from Tianjin Kemio Chemical Reagent Co., Ltd. Lanthanum nitrate ($La(NO_3)_3$) was purchased from Sinopharm Chemical Reagent Co., Ltd.

2.2. Experimental instruments

Ultrasonic cleaner (KQ5200E, China Co. Ltd), FTIR spectrometer (Nicolet IS5, Thermo Fisher Scientific, USA), optical microscope (OPTEC-BK5000, China Co. Ltd), TG analysis (TG, Q600SDT, TA, USA), scanning electron microscope (SEM, JSM-6460LV, JEOL, Japan), and Toup View (Toup View Technology Co., Ltd., China Ltd) were used in this study.

2.3. Experimental methods

2.3.1. Modification of SiO_2

The modification of SiO_2 was carried out according to previous reports with slight modifications (Khan *et al.* 2019). SiO_2 (3 wt%) was added to the CTAB aqueous solution (10^{-2} mol/L) and stirred for 4 h at 25 °C to ensure the adsorption of CTAB on the surface of SiO_2. The precipitate was then collected by centrifugation at a speed of 9,000 rpm and washed three times with deionized water to remove excess CTAB. Finally, the precipitate was dried at 80 °C for 10 h.

2.3.2. Preparation of O/W Pickering emulsions

SA was completely dissolved in deionized water at 80 °C using mechanical stirring to prepare a 0.8% aqueous solution of SA. Then, modified SiO_2 of different quality was added to the 0.8 wt% SA aqueous solution, and the mixture was ultrasonic

oscillated at 2,450 Hz for 5 min to obtain a continuous phase. Kerosene and P204 were mixed in 3:7, 4:6, 5:5, 6:4, and 7:3 ratios as the dispersed phase of Pickering emulsions. The dispersed phase was mixed with the continuous phase in a ratio of 4:6 and then shaken for 30 s to form O/W Pickering emulsions. The type of emulsion was determined by performing a 'dropping' experiment (Binks & Lumsdon 2000). The prepared emulsions were dropped into distilled water, and if they could be dispersed in water, it was determined to be O/W type. If the droplet remained intact, it was determined to be W/O type.

2.3.3. Preparation of PEHGs

The O/W Pickering emulsions were prepared using the above method, and then the Pickering emulsions were dropped in containing 5 wt% $CaCl_2$ solution for 24 h at 4 °C. Following the cross-linking, there was no significant oil-phase leakage from PEHGs. Then, the PEHGs were washed three times with deionized water to remove the oil phase and $CaCl_2$ on the surface. The blank group is the SA hydrogel that does not encapsulate the extraction. The flow chart of the specific preparation of PEHGs is shown in Figure 1.

To compare the adsorption effect, SA hydrogels (HGs) without extraction were prepared as the control group.

2.3.4. La(III) adsorption experiment

The adsorption of PEHGs on La(III) was studied in batch adsorption experiments. Adsorption experiments were conducted by immersing 0.5 g of PEHGs into 50 mL lanthanum solution, and then it was shaken (60 times/min) at a constant temperature. On the extraction of La(III), the effects of varying pH, extractant concentration, and starting concentration were investigated. The absorbance value of the solution was detected by using Arsenazo III UV spectrophotometry (Savvin *et al.* 1972; Pu *et al.* 2002), and the La(III) concentration was calculated by the standard equation $A = 0.2786c–0.1539$ ($n = 6$, $R^2 = 994$). The extraction amount and the extraction rate of lanthanum by PEHGs according to the following equation are calculated:

$$q_e = \frac{(c_0 - c_e) \times V}{w}$$

$$\text{Extraction} = \frac{c_0 - c_e}{c_0} \times 100\%$$

where c_0 (mg/mL) is the initial concentration of lanthanum in the solution, and c_e (mg/mL) is the equilibrium adsorption concentration. V (mL) is the volume of the lanthanum solution, and w (g) is the weight of PEHGs.

Subsequently, the desorption experiment of La(III) was carried out. Around 0.3 g of PEHGs adsorbed with La(III) was soaked in 30 ml of 0.1 mol/L HNO_3 solution for 10 h. Afterwards, the PEHGs were washed with deionized water until pH > 5. The washed samples were used for the next step of adsorption.

2.3.5. Characterization of PEHGs

The size and shape of the emulsified Pickering emulsion droplets were observed with an optical microscope, and the encapsulation of the extractant was analyzed by FTIR spectroscopy and TG. To investigate the microstructure of PEHGs, a SEM

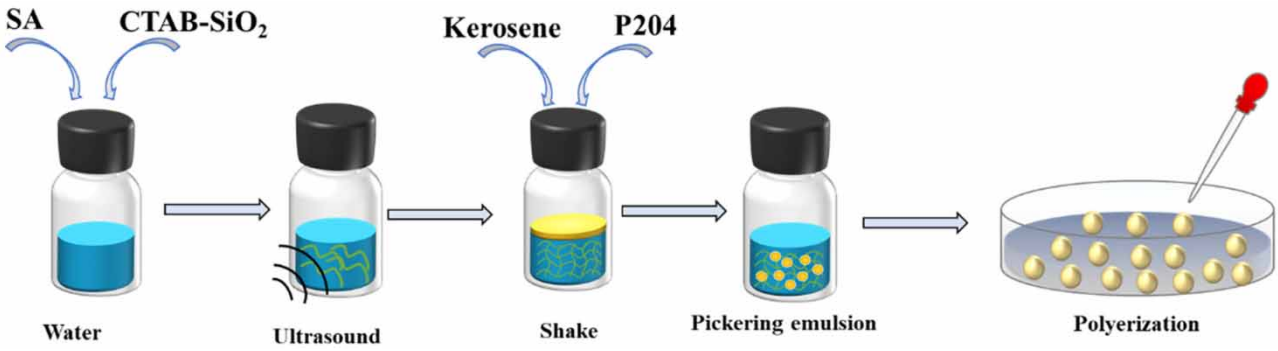

Figure 1 | Preparation of SA PEHGs.

was employed to observe and record the results after vacuum freeze drying. The FTIR spectra of PEHGs before and after adsorption were recorded in a transmission mode.

3. RESULTS AND DISCUSSION

3.1. Characterization

3.1.1. Characterization of silica modification

Since the super-hydrophilic SiO_2 cannot be adsorbed at the oil–water interface, it cannot stabilize the Pickering emulsions. However, the addition of cationic surfactants could cooperate with silica to stabilize Pickering emulsions (Binks *et al.* 2007). This paper stabilized the Pickering emulsions by modifying SiO_2 with cationic surfactant CTAB. The presence of CTAB was further confirmed via FTIR analysis as shown in Figure 2(a). CTAB-modified silica (CTAB-SiO_2) has almost similar absorption peaks as SiO_2. A strong peak at 1,102 cm^{-1} is attributed to the Si–O–Si anti-symmetrical stretching vibration, while the

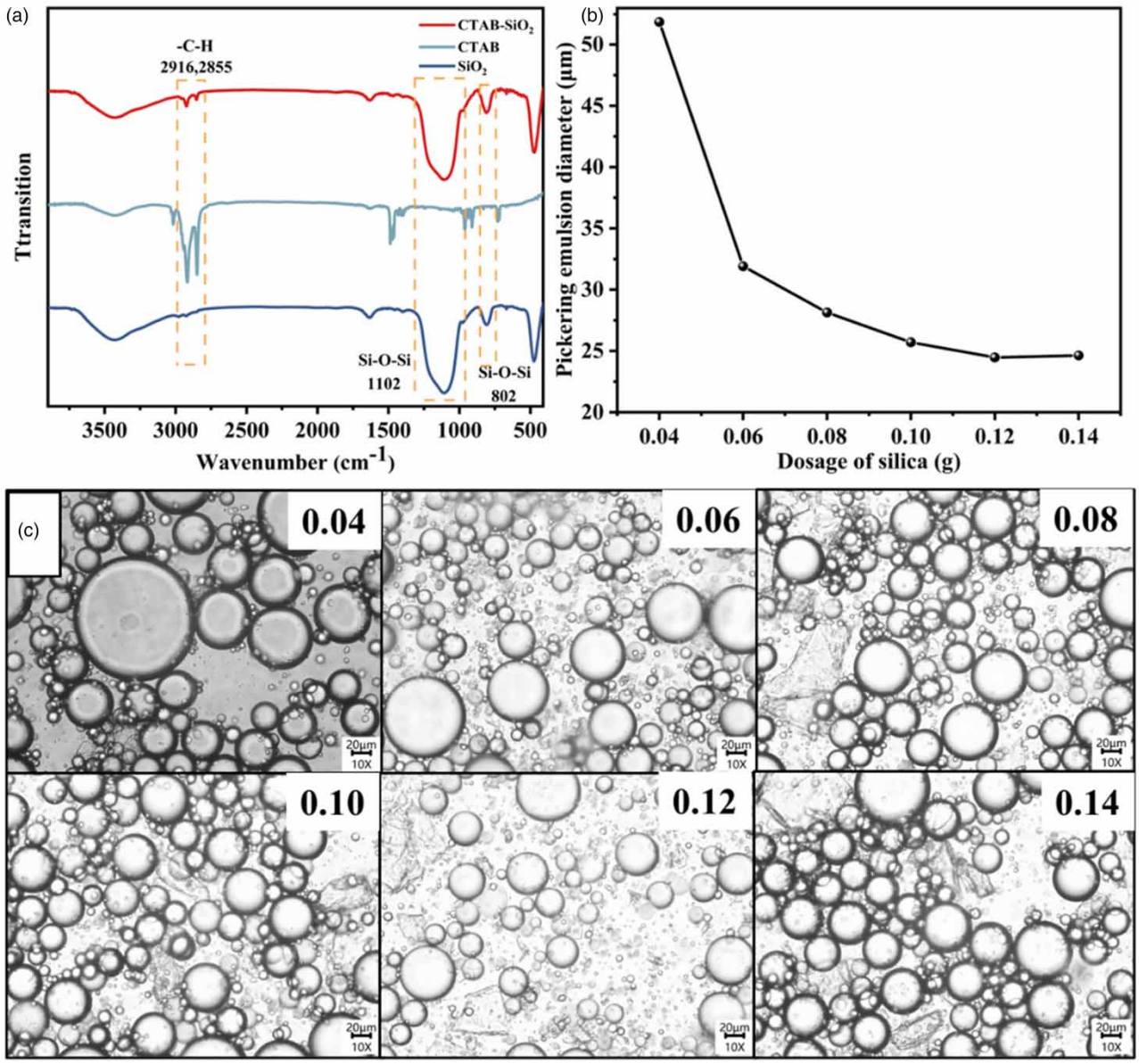

Figure 2 | (a) FTIR spectrum of SiO_2 and CTAB-modified SiO_2. (b) Particle size distribution of Pickering emulsions stabilized by CTAB-SiO_2 at different concentrations. (c) Micrographs of 0.04–0.14 g SiO_2-stabilized Pickering emulsions.

Si–O–Si symmetrical stretching is detected at 802 cm^{-1}. The typical C–H stretching vibrations were found at 2,855 and 2,916 cm^{-1}, which correspond to the $-CH_2$ and $-CH_3$ peaks in CTAB. This is consistent with the previously reported phenomenon of the modification of SiO_2 (Saman *et al.* 2020).

3.1.2. Characterization of Pickering emulsions

The effects of particle concentrations of 0.4–1.4 wt% on the stability of Pickering emulsions were studied by using CTAB-SiO_2 to stabilize the emulsions. All emulsions were O/W emulsions, and the emulsions' particle size observed by the optical microscope is shown in Figure 2(c). The figure shows that as particle concentration increases, the particle size of the emulsions reduces progressively and eventually tends to remain stable. The particle size distribution is shown in Figure 2(b). The concentration of CTAB-SiO_2 increased from 0.4 to 1.4 wt%, and the average particle size of the emulsions decreased from 52 to 24 μm. Specifically, the increase in particle concentration allows more nanoparticles to reach the oil–water interface, which in turn expands the area of the interface and reduces the size of the emulsions. The average size of the emulsions is also shown to stabilize at 1.0 wt% of particle concentration, so CTAB-SiO_2 with a particle concentration of 1.0 wt% is selected to stabilize the O/W emulsions.

3.1.3. Characterization of PEHGs

The continuous phase of Pickering emulsions was SA polymeric monomer, the dispersed phase was extractant, and the cross-linking agent was $CaCl_2$. A three-dimensional network hydrogel encapsulating the P204 extractant was formed through a chemical reaction, and its cross-linking mode is shown in Figure 3(a). The H^+ in the carboxyl functional groups of alginate is replaced with Ca^{2+}, which are then linked together to form hydrogels.

The infrared images of HGs, P204, and PEHGs are shown in Figure 4(a). It can be seen that HGs and PEHGs have similar infrared characteristic peaks. In the infrared spectrum of P204, the methyl peak is located between 2,858 and 2,964 cm^{-1}, the P = O peak is located at 1,235 cm^{-1}, and the P–OH peak is located at 810 cm^{-1}. Additionally, PEHGs show these P204-specific peaks, demonstrating that P204 was successfully wrapped in PEHGs.

The encapsulation ratio of PEHGs was determined using the thermal stability curves of HGs and PEHGs, as shown in Figure 5(a). The TGA of PEHGs exhibited a three-stage weight loss. The first stage, occurring between 0 and 80 °C, primarily entailed water evaporation. The second stage, spanning from 80 to 158 °C, predominantly involved the degradation of SA, which corresponds to the TGA curve of HGs. The third stage, ranging from 158 to 271 °C, resulted in a weight loss of 36.84% during the breakdown of kerosene/P204. The extractant's weight loss was consistent with the expected value of 40%, indicating that it was successfully encapsulated in PEHGs.

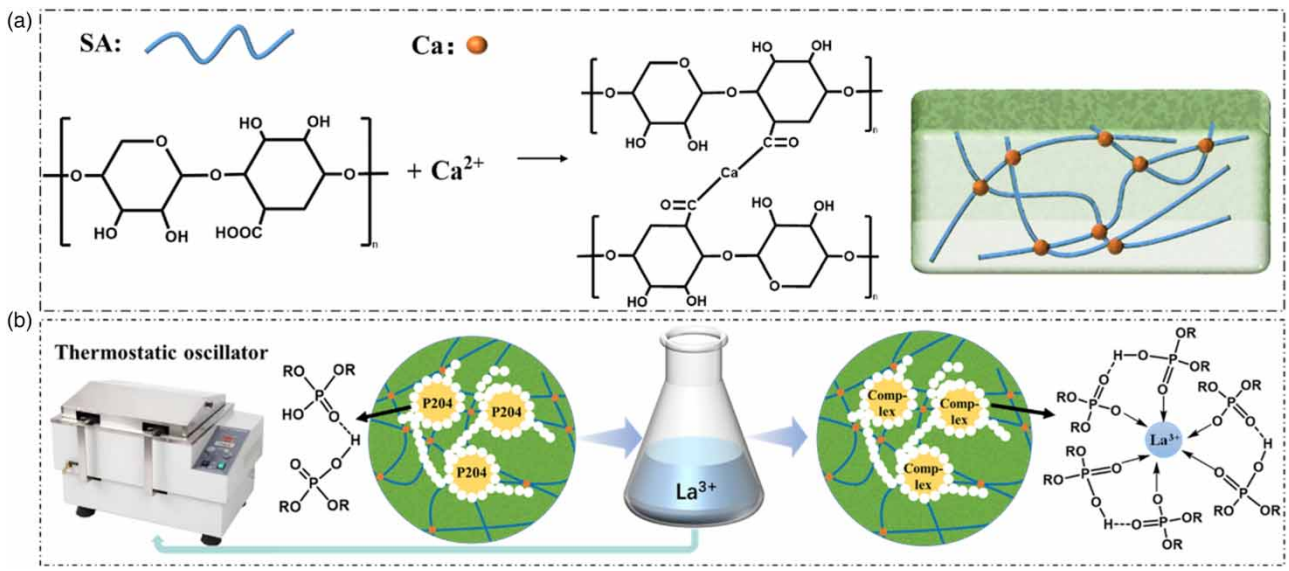

Figure 3 | (a) Cross-linking mechanism diagram of SA and calcium ions, and (b) PEHGs extraction mechanism of La(III).

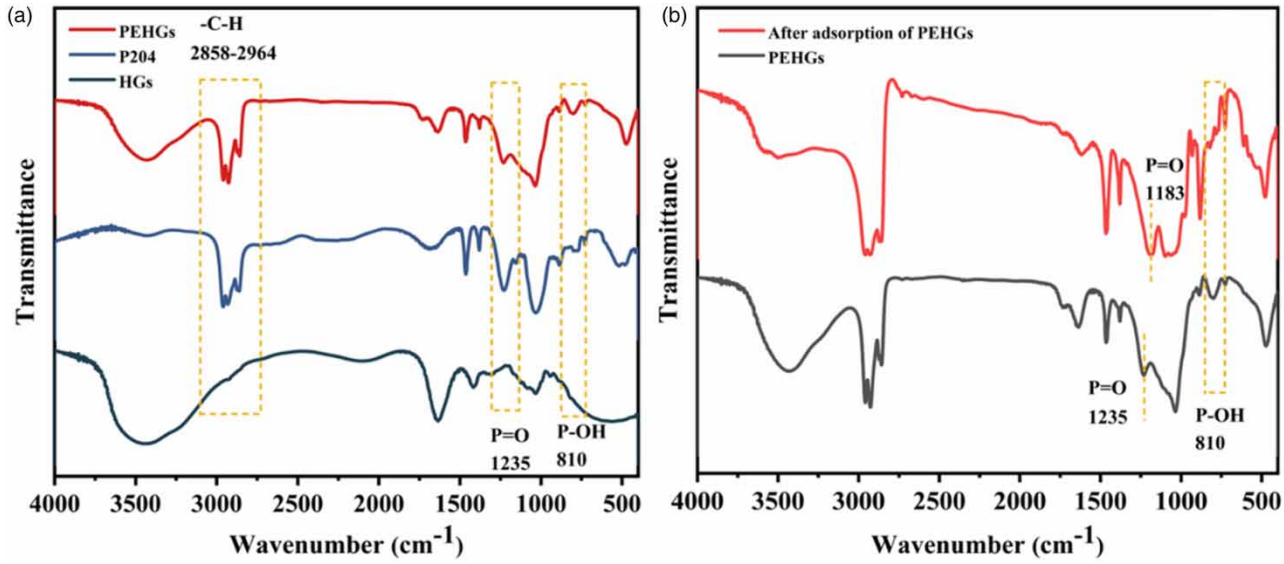

Figure 4 | (a) FTIR spectra of hydrogels, P204, and PEHGs. (b) FTIR spectra of PEHGs before and after adsorption.

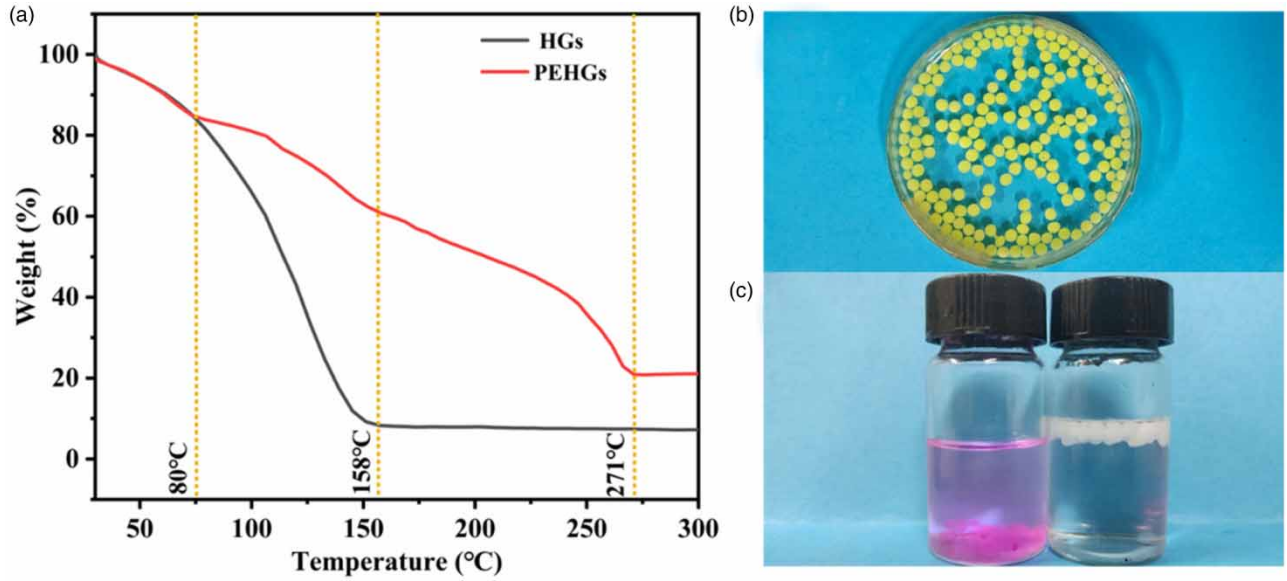

Figure 5 | (a) TGA curves of HGs and PEHGs. (b) Curcumin-containing PEHGs. (c) Rhodamine-B stained hydrogel and PEHGs.

To verify that the extractant was encapsulated in SA hydrogels, and curcumin was dissolved in kerosene to prepare the oil phase. The prepared PEHGs are shown in Figure 5(b), and it can be seen that the prepared PEHGs are yellow and have no obvious leakage.

Moreover, Rhodamine-B was dissolved in the SA aqueous solution to prepare hydrogel, and the results were compared with PEHGs. Figure 5(c) shows that the hydrogels without the extractant were submerged at the bottom, while the PEHGs with the extractant were floated on the surface. Because the density of the oil phase is lower than that of water, the PEHGs are less dense and therefore float on the surface. This phenomenon indicated the successful encapsulation of the extractant.

Figure 6 shows SEM images of HGs and PEHGs. Some smooth layered structures can be seen clearly from the cross-sectional view of the SEM images (Figure 6(a)). The SA hydrogel's weak mechanical properties and the breakdown

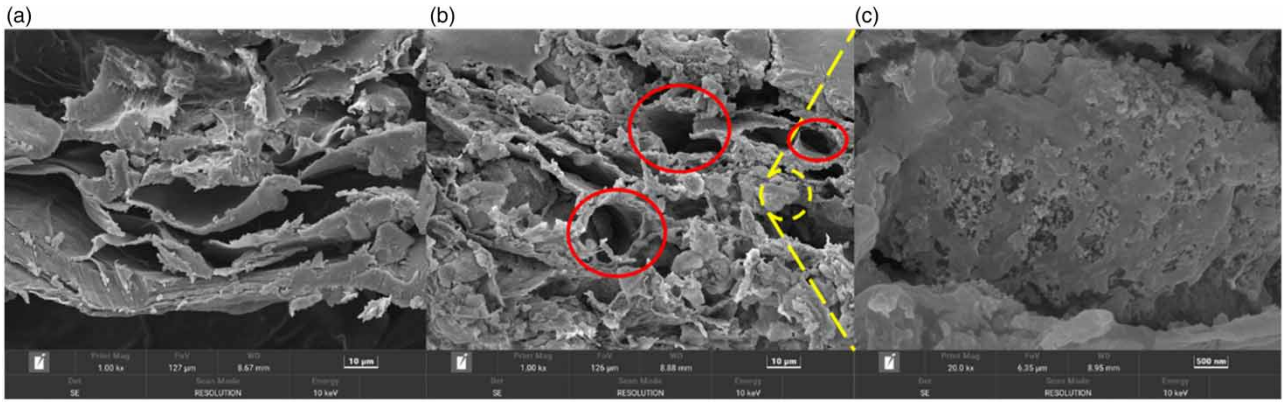

Figure 6 | SEM images of (a) HGs (1,000×), (b) PEHGs (1,000×), and (c) SEM images magnified in a yellow circle (20,000×).

of the network structure during vacuum drying resulted in this structure. In the microscopic cross-section diagram of PEHGs (Figure 6(b)), some 20 μm closed holes emerged after the oil phase extracted from the PEHGs (red circle in Figure 6(b)), because the presence of SiO_2 on the surface of the Pickering emulsion droplets improved the mechanical characteristics of the hydrogels and resulted in the formation of isolated holes. Compared with hydrogels, the surface of PEHGs is rougher due to the aggregation of SiO_2. When the magnification was adjusted to 20,000 (Figure 6(c)), the dense nano-SiO_2 on the PEHGs surface was clearly evident.

3.2. Adsorption mechanism of PEHGs

Figure 3(b) shows the extraction process of lanthanum ions by P204 extractant in PEHGs. This process was achieved by placing an Erlenmeyer flask containing lanthanum ions in an oscillator. SA is a hydrophilic hydrogel that provides a channel for the diffusion of La(III) from the aqueous phase to the oil–water interface, then La(III) complexes with P204 dimer to generate a 6-coordinated $La(HA_2)_3$ complex (Zheng *et al.* 2022). The resultant lanthanum ion complex diffused into the interior of the oil phase, and the unreacted extractant diffused to the oil–water interface to continue the reaction. The FTIR spectrum also proved its complexation mechanism, and Figure 4(b) shows the infrared spectrum of PEHGs before and after adsorption. It can be seen that the P–OH characteristic peak at 810 cm^{-1} after adsorption is significantly weakened, indicating that H^+ in P–OH of P204 is replaced by La(III), and the P = O characteristic absorption peak after adsorption moved from 1,235 to 1,183 cm^{-1}. This displacement change indicated that P204 formed a P = O → La coordination bond with the lanthanum ion. This phenomenon was confirmed by the adsorption mechanism (Figure 3(b)).

3.3. Adsorption experiments of La(III)

3.3.1. Study on adsorption conditions

(1) Effect of extraction time on adsorption content

To study the effect of adsorption time on lanthanum adsorption, 0.5 g of PEHGs were added into the lanthanum solution at an initial concentration of 1 mg/mL (50 mL). As shown in Figure 7(a), the adsorption content increased as the adsorption time increased and reached equilibrium after 14 h, and the maximum adsorption amount was 38.05 mg/g. Therefore, in the subsequent experiments, the adsorption time was set as 14 h. As a control, the HGs without encapsulating P204 reached adsorption equilibrium within 3 h, and the adsorption amount was only 5.42 mg/g. This indicated that the adsorption of PEHGs mainly depends on the extraction of P204. The equilibrium time was longer when compared to the adsorption capacity of La(III) by PEHGs and the impregnated resin (İnan *et al.* 2018; Yarahmadi *et al.* 2023) adsorption capacity of 7.324 and 11.1 mg/g, but the extraction capacity was greatly enhanced.

(2) Effect of pH on adsorption content

The effect of the initial pH was evaluated by varying the solution pH from 1.5 to 4.5 using NaOH and HNO_3 to adjust the pH. Figure 7(b) shows the extraction capacity as a function of pH for 14 h extraction time, the maximum adsorption capacity

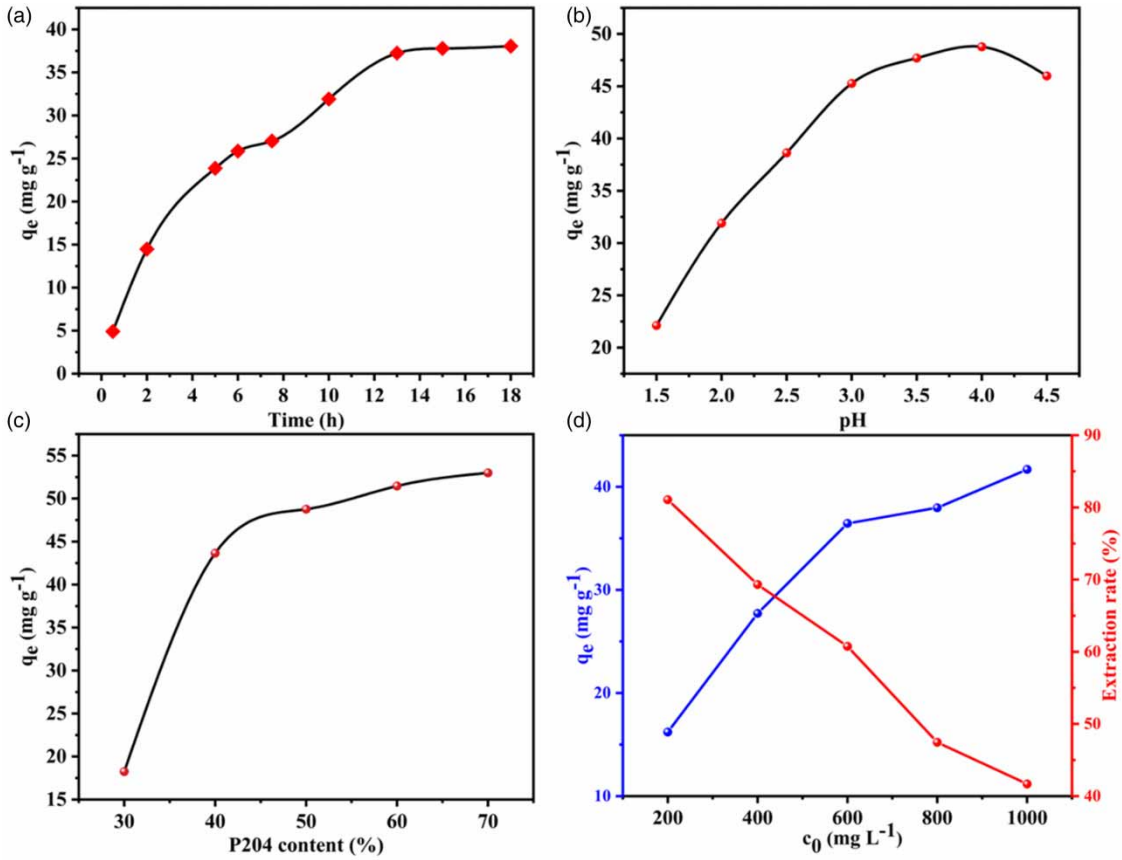

Figure 7 | Influence of different conditions on extraction. (a) Time, (b) pH value, (c) extractant concentration, and (d) initial concentration.

was obtained as 48.77 mg/g at pH 4, and then gradually decreased as the pH increased. The adsorption mechanism of PEHGs on La(III) was a cation exchange reaction, and the reaction equation was shown as follows:

$$La^{3+} + 3(HA)_2 \rightarrow La(HA_2)_3 + 3H^+$$

HA is P204, $(HA)_2$ is a dimer of P204, and La $(HA_2)_3$ is a complex of La(III) and P204.

When the pH < 4, the concentration of H^+ decreases with the increase of pH, leading to the positive direction of the reversible reaction, which is beneficial for the complexation of La(III) with the extractant. When pH > 4, La(III) in the solution may form a complex with OH^- in the solution, thus hindering the complexation reaction between the extractant and La(III) (El-Sofany 2008).

(3) Effect of P204 concentration on adsorption content

Kerosene was selected as a diluent, and extractants with volume fractions of 30, 40, 50, 60, and 70% were configured as organic phases. The effect of extractant concentration on the extraction of La(III) was studied under the condition of pH 4 and an extraction time of 14 h.

The results are shown in Figure 7(c), and the amount of La(III) extracted increases dramatically as the concentration of the extractant increases. However, it seems that raising the content of P204 above 40% did not lead to a significant improvement in adsorption capacity for La(III). This could be owing to P204's high viscosity, which reduces the diffusion rate of La(III) in the organic phase, resulting in a decrease in La(III) adsorption. Therefore, more focus was on the concentration of P204 at 40% to maximize adsorption capacity.

(4) Effect of initial solution concentration on adsorption capacity

PEHGs adsorbed La(III) solutions with different initial concentrations, as shown in Figure 7(d). As the initial concentration of La(III) increases, the adsorption capacity of the PEHGs also increases. Intuitively, larger concentrations result in faster transfer rates and more frequent collisions, which are necessary for chemical reactions to occur. However, it is interesting to note that as the starting concentration increased, the extraction rate declined. This phenomenon is consistent with previous reports (El-Sofany 2008).

3.3.2. Adsorption isotherms

To better understand the adsorption properties of La(III) toward PEHGs, the adsorption isotherm of PEHGs has been further investigated. The equilibrium adsorption capacity of PEHGs was tested at 298, 303, 308, 313, and 318 K, respectively, when the initial concentration of La(III) was 200–1,000 mg/L, and the Langmuir and Freundlich models were established to fit the experimental data. The original equations of the Langmuir model (Langmuir 1916) and Freundlich model (Freundlich 1937) are as follows:

$$q_e = \frac{q_0 K_L c_e}{1 + K_L c_e}$$

$$q_e = K_F c_e^{\left(\frac{1}{n}\right)}$$

Later, in order to analyze the data more easily, the Langmuir model (Bao *et al.* 2016) and the Freundlich model (Nanta *et al.* 2018) were transformed into linear equations, as shown in the following formula:

$$\frac{c_e}{q_e} = \frac{1}{q_0 K_L} + \frac{c_e}{q_0}$$

$$\log q_e = \frac{1}{n} \log c_e + \log K_F$$

where c_e is the equilibrium concentration of La(III), q_e is the adsorption capacity in an equilibrium state, q_0 is the monolayer adsorption capacity in the Langmuir model, K_L is the Langmuir equilibrium constant, K_F is the Freundlich equilibrium constant, and n is the homogeneous factor.

The equilibrium data results were fitted to the linear Langmuir and Freundlich models. Figure 8(a) and 8(b) shows the linear plots of c_e/q_e versus c_e and $\log q_e$ versus $\log c_e$ at different temperatures, respectively. It can be seen from the figure that at the same concentration, the adsorption capacity increases with the increase in temperature. The corresponding constants and the coefficient of determination (R^2) calculated by the two isotherm models are listed in Table 1. It was found that the experimental data were fitted well by the Langmuir and Freundlich adsorption isotherm models, but the linear correlation performances were different. The Langmuir adsorption isotherm was more consistent with the experimental data, and its correlation coefficient was $R^2 > 0.9925$. The results showed that the adsorption of La(III) on PEHGs is mainly chemisorption, and the Langmuir adsorption isotherm model is more suitable for studying the equilibrium adsorption of La(III) on PEHGs.

Further analysis of the Langmuir equation was carried out, and the dimensionless equilibrium parameter (R_L) was calculated and its calculation formula is as follows:

$$R_L = \frac{1}{K_L c_0}$$

The R_L indicates the nature of the isotherm accordingly: $0 < R_L < 1$ shows favorable adsorption, $R_L = 1$ indicates linear adsorption, and $R_L = 0$ indicates irreversible adsorption. At the temperature of 298–318 K, when c_0 changes from 200 to 1,000 mg/L, the range of R_L value is 0.007–0.229. This result indicated that the removal of La(III) using PEHGs is a favorable adsorption process.

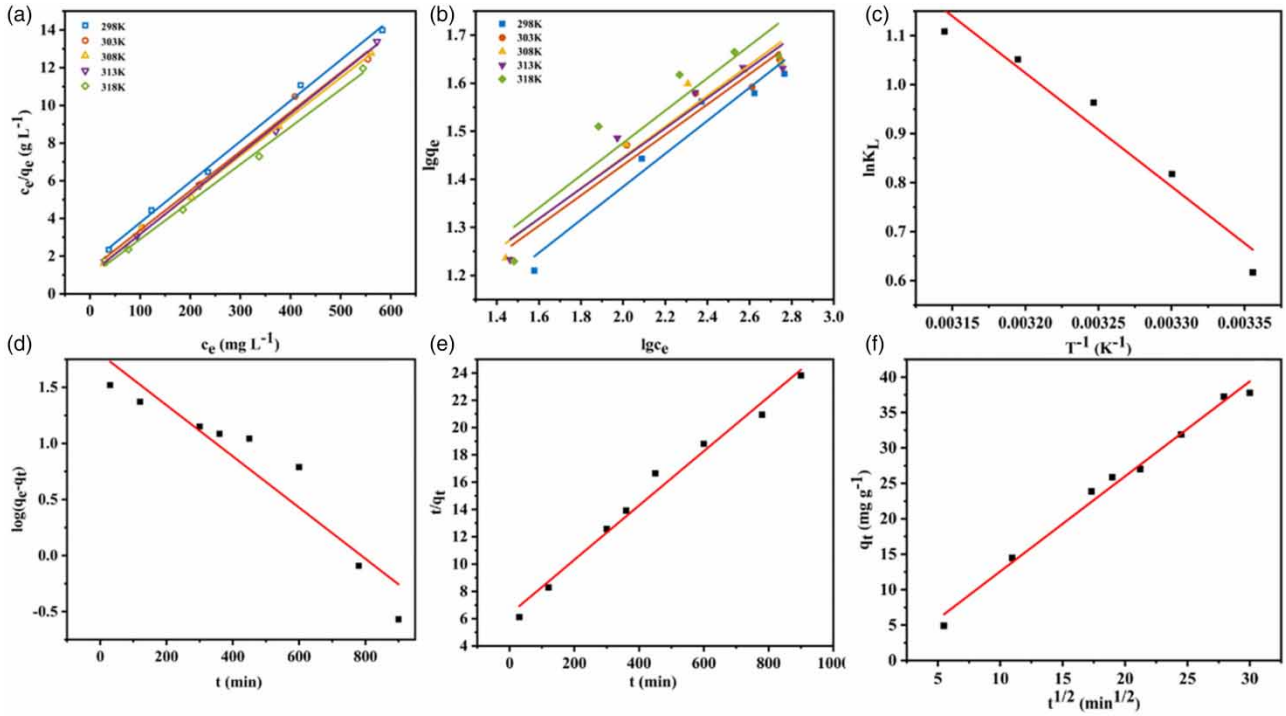

Figure 8 | (a) Langmuir adsorption isotherm, (b) Freundlich adsorption isotherm, (c) thermodynamic Curves, (d) pseudo-first-order kinetics, (e) pseudo-second-order kinetics, and (f) internal diffusion model.

Table 1 | Corresponding constants of Langmuir adsorption isotherm and Freundlich adsorption isotherm at different temperatures

	Langmuir adsorption isotherm			Freundlich adsorption isotherm		
Temperature (K)	q_0 (mg g^{-1})	K_L (L $mmol^{-1}$)	R^2	K_F (mg $g^{-1)}$	n	R^2
298	46.34	1.853	0.9969	4.98	2.91	0.9526
303	47.82	2.265	0.9925	6.28	3.17	0.9538
308	48.24	2.620	0.9988	6.37	3.12	0.9453
313	46.97	2.862	0.9986	6.55	3.12	0.9288
318	50.35	3.030	0.9964	6.33	2.97	0.8675

3.3.3. Adsorption thermodynamics

Based on the adsorption equilibrium constants determined from the Langmuir isotherm, the thermodynamic parameters can be computed by examining the adsorption thermodynamics through the application of the following equations, such as ΔG, ΔH, and ΔS (Anastopoulos & Kyzas 2016).

$$\Delta G = \Delta H - T\Delta S$$

$$\Delta G = -RT\ln K_L$$

where K_L is the equilibrium constant obtained from the Langmuir isotherm, R is the gas constant (8.314 J/(mol·ΔK)), and T is the absolute temperature (K).

Combining the above formulas, the following formula is obtained:

$$\ln K_L = \frac{\Delta S}{R} - \frac{\Delta H}{RT}$$

As shown in Figure 8(c), it reflects the linear plot of ln K_L and $1/T$. Thus, ΔH and ΔS could be calculated from the slope and intercept of the linear plot of ln K_L and $1/T$, and the relevant parameters are listed in Table 2. The positive value ΔH indicated that the reaction is endothermic. With increasing temperature, the reaction progresses with greater efficiency, thereby facilitating the extraction process. The positive value of ΔS indicated that the randomness of the solid/solution interface increases during the adsorption of La(III) by PEHGs. A negative value of ΔG indicated in all cases that the reaction of P204 to extract La(III) is spontaneous.

3.3.4. Adsorption kinetics

The graph presented above illustrates the adsorption quantity of PEHGs on La(III) over time. It is evident that the adsorption of PEHGs on La(III) attains equilibrium after a duration of 14 h. Kinetic modeling for La(III) adsorption on PEHGs was investigated using three common models, including pseudo-first-order (Xu *et al.* 2020), pseudo-second-order (Ho 2006), and intraparticle diffusion kinetic equations (Wang & Guo 2022), and its linear formula is as follows:

$$\log(q_e - q_t) = \log q_e - \frac{k_1}{2.303} t$$

$$\frac{t}{q_t} = \frac{1}{k_2 q_e^2} + \frac{1}{q_e} t$$

$$q_t = k_{int} t^{0.5} + C$$

Figure 8(d)–8(f) presents the fitting lines of three different models: the pseudo-first-order kinetic model, the pseudo-second-order kinetic model, and the internal diffusion model. The kinetic parameters are summarized in Table 3.

Upon examining the fitting line and relevant data, it was evident that the pseudo-second-order kinetic model aligns well with the experimental data, and the calculated theoretical saturation quantities $q_{e,cal}$ (50.25 mg/g) were in good agreement with the experimental values. Hence, it could be concluded that the pseudo-second-order kinetic model is more suitable for explaining the adsorption process of La(III) on PEHGs, indicating a chemisorption mechanism.

The correlation coefficient $R^2 = 0.9886$ of the straight line fitted by the internal diffusion model fits the experimental data, demonstrating that internal diffusion was involved in adsorption. This phenomenon and the increase in the concentration of

Table 2 | Thermodynamic parameters of La (III) adsorption at different temperatures

Temperature (K)	ΔH (kJ mol^{-1})	ΔS (kJ mol^{-1} K^{-1})	ΔG (kJ mol^{-1})
298	19.266	0.070	−1.643
303			−1.994
308			−2.345
313			−2.695
318			−3.046

Table 3 | Dynamic model parameters

Pseudo-first-order kinetic			Pseudo-second-order kinetic			Inter diffusion model	
k_1	$q_{e,\,cal}$ (mg g^{-1})	R^2	k_2	$q_{e,\,cal}$ (mg g^{-1})	R^2	k_{int}	R^2
0.005	62.77	0.8961	0.0006	50.25	0.9838	1.341	0.9886

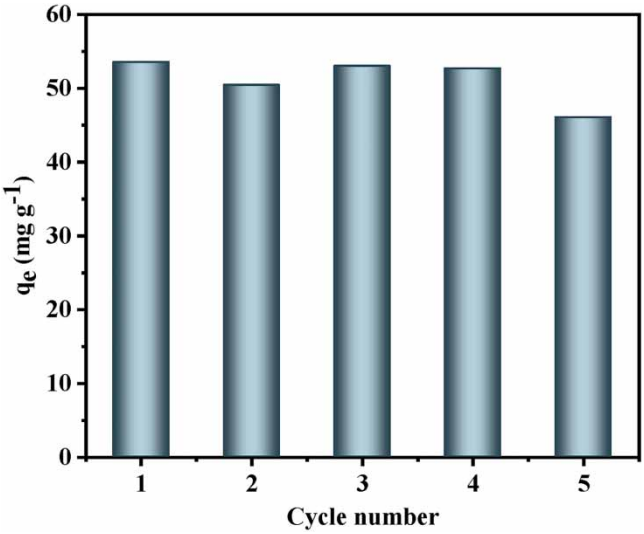

Figure 9 | The adsorption capacity of La(III) by recycling PEHGs.

P204 mentioned above would increase the viscosity of the oil phase, resulting in the diffusion rate of La(III) reducing the adsorption efficiency of La(III).

3.3.5. Adsorption/desorption of PEHGs

To assess the reusability of PEHGs, La(III) was desorbed in PEHGs using 0.1 mol/L HNO_3, and the extraction process was repeated. Figure 9 illustrates the changes in the adsorption effect of PEHGs after five adsorption cycles. The figure revealed that after the fifth adsorption cycle, the adsorption effect of the pellets exhibited a noticeable decline, although its adsorption capacity remained above 85%. The decrease in adsorption amount could be attributed to the incomplete desorption of La(III). The aqueous phase was always clear throughout the experiment, indicating that the PEHGs did not leak solvent across repeated cycles.

4. CONCLUSION

In summary, the modified silica could stabilize the emulsions to prepare PEHGs that contain the P204, and no obvious leakage of the extraction agent was seen. The adsorption capacity of La(III) by PEHGs was up to 48 mg/g. The adsorption isotherm of PEHGs on La(III) is in good agreement with the Langmuir model, and the adsorption process was a spontaneous endothermic process. The pseudo-second-order kinetic model could explain the adsorption process of La(III) on PEHGs. Through the internal diffusion model, it has been found that the adsorption process was related to internal diffusion. The results of adsorption/desorption experiments showed that PEHGs could be recycled, which indicated that this work provided an efficient and clean method for recovering rare earth metals in an aqueous solution.

ACKNOWLEDGEMENTS

This work was supported by the Xi'an University of Science and Technology, Grant/Award Number: 19023.

DATA AVAILABILITY STATEMENT

All relevant data are included in the paper or its Supplementary Information.

CONFLICT OF INTEREST

The authors declare there is no conflict.

REFERENCES

Ahmed, E. M. 2015 Hydrogel: Preparation, characterization, and applications: A review. *Journal of Advanced Research* **6** (2), 105–121. http://dx.doi.org/10.1016/j.eurpolymj.2021.110935.

Anastopoulos, I. & Kyzas, G. Z. 2016 Are the thermodynamic parameters correctly estimated in liquid-phase adsorption phenomena? *Journal of Molecular Liquids* **218**, 174–185. http://dx.doi.org/10.1016/j.molliq.2016.02.059.

Bao, S., Tang, Y., Zhang, Y. & Liang, L. 2016 Recovery and separation of metal ions from aqueous solutions by solvent-impregnated resins. *Chemical Engineering & Technology* **39** (8), 1377–1392. http://dx.doi.org/10.1002/ceat.201500324.

Binks, B. P. & Lumsdon, S. 2000 Influence of particle wettability on the type and stability of surfactant-free emulsions. *Langmuir* **16** (23), 8622–8631. http://dx.doi.org/10.1021/la000189s.

Binks, B. P., Rodrigues, J. A. & Frith, W. J. 2007 Synergistic interaction in emulsions stabilized by a mixture of silica nanoparticles and cationic surfactant. *Langmuir* **23** (7), 3626–3636. http://dx.doi.org/10.1021/la0634600.

Dong, C., Gao, J., Zhao, Y., Zhao, W., Ning, K., Wu, P. & He, Y. 2023 Preparation of Pickering emulsion hydrogels containing indium (III) extractants and their indium (III) recycling properties. *Clean Technologies and Environmental Policy*, 1–11. http://dx.doi.org/10.1007/s10098-023-02545-9.

El-Sofany, E. 2008 Removal of lanthanum and gadolinium from nitrate medium using Aliquat-336 impregnated onto Amberlite XAD-4. *Journal of Hazardous Materials* **153** (3), 948–954. http://dx.doi.org/10.1016/j.jhazmat.2007.09.046.

Freundlich, H. 1937 Some recent work on gels. *Journal of Physical Chemistry* **41** (7), 901–910. http://dx.doi.org/10.1021/j150385a001.

Gao, J., Dong, C., Zhao, Y., Liang, Y., Ning, K., Yang, L. & He, Y. 2023 Removal of zinc ions from aqueous solution using zinc extractant-encapsulated hydrogels formed by Pickering emulsion technique. *Environment, Development and Sustainability* 1–17. http://dx.doi.org/10.1007/s10668-023-03158-4.

Ho, Y.-S. 2006 Second-order kinetic model for the sorption of cadmium onto tree fern: A comparison of linear and non-linear methods. *Water Research* **40** (1), 119–125. http://dx.doi.org/10.1016/j.watres.2005.10.040.

Huang, X., Wu, H., Wang, Z., Luo, Y. & Song, H. 2017 High resolution of racemic phenylalanine with dication imidazolium-based chiral ionic liquids in a solid-liquid two-phase system. *Journal of Chromatography A* **1479**, 48–54. http://dx.doi.org/10.1016/j.chroma.2016.12.012.

İnan, S., Tel, H., Sert, Ş., Çetinkaya, B., Sengül, S., Özkan, B. & Altaş, Y. J. H. 2018 Extraction and separation studies of rare earth elements using Cyanex 272 impregnated Amberlite XAD-7 resin. *Hydrometallurgy* **181**, 156–163. http://dx.doi.org/10.1016/j.hydromet.2018.09.005.

Khan, A. M., Shafiq, F., Khan, S. A., Ali, S., Ismail, B., Hakeem, A. S., Rahdar, A., Nazar, M. F., Sayed, M. & Khan, A. R. 2019 Surface modification of colloidal silica particles using cationic surfactant and the resulting adsorption of dyes. *Journal of Molecular Liquids* **274**, 673–680. http://dx.doi.org/10.1016/j.molliq.2018.11.039.

Kobayashi, T., Yoshimoto, M. & Nakao, K. 2010 Preparation and characterization of immobilized chelate extractant in PVA gel beads for an efficient recovery of copper (II) in aqueous solution. *Industrial & Engineering Chemistry Research* **49** (22), 11652–11660. http://dx.doi.org/10.1021/ie101113s.

Kumar, B. N., Radhika, S. & Reddy, B. R. 2010 Solid–liquid extraction of heavy rare-earths from phosphoric acid solutions using Tulsion CH-96 and T-PAR resins. *Chemical Engineering Journal* **160** (1), 138–144. http://dx.doi.org/10.1016/j.cej.2010.03.021.

Langmuir, I. 1916 The constitution and fundamental properties of solids and liquids. Part I. Solids. *Journal of the American Chemical Society* **38** (11), 2221–2295. http://dx.doi.org/10.1021/ja02268a002.

Lili, Z. & Ji, C. 2011 Adsorption of Ce (IV) in nitric acid medium by imidazolium anion exchange resin. *Journal of Rare Earths* **29** (10), 969–973. http://dx.doi.org/10.1016/s1002-0721(10)60580-7.

Mohammedi, H., Miloudi, H., Tayeb, A., Bertagnolli, C. & Boos, A. 2019 Study on the extraction of lanthanides by a mesoporous MCM-41 silica impregnated with Cyanex 272. *Separation and Purification Technology* **209**, 359–367. http://dx.doi.org/10.1016/j.seppur.2018.07.035.

Nanta, P., Kasemwong, K. & Skolpap, W. 2018 Isotherm and kinetic modeling on superparamagnetic nanoparticles adsorption of polysaccharide. *Journal of Environmental Chemical Engineering* **6** (1), 794–802. http://dx.doi.org/10.1016/j.jece.2017.12.063.

Neagu, V., Avram, E. & Lisa, G. 2010 N-methylimidazolium functionalized strongly basic anion exchanger: Synthesis, chemical and thermal stability. *Reactive and Functional Polymers* **70** (2), 88–97. http://dx.doi.org/10.1016/j.reactfunctpolym.2009.10.009.

Ngomsik, A.-F., Bee, A., Talbot, D. & Cote, G. 2012 Magnetic solid–liquid extraction of Eu (III), La (III), Ni (II) and Co (II) with maghemite nanoparticles. *Separation and Purification Technology* **86**, 1–8. http://dx.doi.org/10.1016/j.seppur.2011.10.013.

Panda, R., Jha, M. K., Hait, J., Kumar, G., Singh, R. J. & Yoo, K. 2016 Extraction of lanthanum and neodymium from leach liquor containing rare earth metals (REMs). *Hydrometallurgy* **165**, 106–110. http://dx.doi.org/10.1016/j.hydromet.2015.10.019.

Pu, Q., Liu, P., Hu, Z. & Su, Z. 2002 Spectrophotometric determination of the sum of rare earth elements by flow-injection on-line preconcentration with a novel aminophosphonic–carboxylic acid resin. *Analytical Letters* **35** (8), 1401–1414. http://dx.doi.org/10.1081/al-120006675.

Puguan, J. M. C., Yu, X. & Kim, H. 2015 Diffusion characteristics of different molecular weight solutes in Ca–alginate gel beads. *Colloids and Surfaces A: Physicochemical and Engineering Aspects* **469**, 158–165. http://dx.doi.org/10.1016/j.colsurfa.2015.01.027.

Radhika, S., Nagaraju, V., Kumar, B. N., Kantam, M. L. & Reddy, B. R. 2012 Solid-liquid extraction of Gd (III) and separation possibilities of rare earths from phosphoric acid solutions using Tulsion CH-93 and Tulsion CH-90 resins. *Journal of Rare Earths* **30** (12), 1270–1275. http://dx.doi.org/10.1016/s1002-0721(12)60219-1.

Ramsden, W. 1904 Separation of solids in the surface-layers of solutions and 'suspensions' (observations on surface-membranes, bubbles, emulsions, and mechanical coagulation). Preliminary account. *Proceedings of the Royal Society of London* **72** (477–486), 156–164. http://dx.doi.org/10.1098/rspl.1903.0034.

Saman, N., Othman, N. S., Chew, L.-Y., Setapar, S. H. M. & Mat, H. 2020 Cetyltrimethylammonium bromide functionalized silica nanoparticles (MSN) synthesis using a combined sol-gel and adsorption steps with enhanced adsorption performance of oxytetracycline in aqueous solution. *Journal of the Taiwan Institute of Chemical Engineers* **112**, 67–77. http://dx.doi.org/10.1016/j.jtice.2020.07.008.

Savvin, S., Petrova, T. & Romanov, P. 1972 Arsenazo III and its analogues – VII: Colour reactions of the rare earth elements with a new reagent – carboxynitrazo. *Talanta* **19** (11), 1437–1441. http://dx.doi.org/10.1016/0039-9140(72)80138-3.

Tokuyama, H., Nakahata, Y., Sato, R., Nagatsu, Y. & Ban, T. 2018 Mechanical and metal adsorption properties of emulsion gel adsorbents composed of PEGDA-co-PEG hydrogels and tri-n-octylamine. *Polymer Bulletin* **75**, 1597–1606. http://dx.doi.org/10.1007/s00289-017-2116-x.

Wang, J. & Guo, X. 2022 Rethinking of the intraparticle diffusion adsorption kinetics model: Interpretation, solving methods and applications. *Chemosphere* **309**, 136732. http://dx.doi.org/10.1016/j.chemosphere.2022.136732.

Xiaoqi, S., Yang, J., Ji, C. & Jiutong, M. 2009 Solvent impregnated resin prepared using task-specific ionic liquids for rare earth separation. *Journal of Rare Earths* **27** (6), 932–936. http://dx.doi.org/10.1016/s1002-0721(08)60365-8.

Xu, C., Shi, S., Dong, Q., Zhu, S., Wang, Y., Zhou, H., Wang, X., Zhu, L., Zhang, G. & Xu, D. 2020 Citric-acid-assisted sol-gel synthesis of mesoporous silicon-magnesium oxide ceramic fibers and their adsorption characteristics. *Ceramics International* **46** (8), 10105–10114. http://dx.doi.org/10.1016/j.ceramint.2019.12.279.

Xu, H., Zhang, L., Pang, Z., Wang, Z., Li, W. & Deng, J. 2022 The study on extraction behavior of [n1888][p507] and TRPO for heavy rare earths. *Minerals Engineering* **176**, 107339. http://dx.doi.org/10.1016/j.mineng.2021.107339.

Yarahmadi, A., Khani, M. H., Nasiri Zarandi, M. & Amini, Y. 2023 Ce(III) and La(III) ions adsorption through Amberlite XAD-7 resin impregnated via CYANEX-272 extractant. *Scientific Reports* **13** (1), 6930. http://dx.doi.org/10.1038/s41598-023-34140-9.

Yuan, S., Liu, Q., Liang, Y., Ning, K., Yu, X. & He, Y. 2021 Dual 3-D networked Pickering emulsion hydrogels encapsulating copper extractants for the recovery of Cu^{2+} from water. *Journal of Environmental Chemical Engineering* **9** (2), 105154. http://dx.doi.org/10.1016/j.jece.2021.105154.

Zhang, Y., Kogelnig, D., Morgenbesser, C., Stojanovic, A., Jirsa, F., Lichtscheidl-Schultz, I., Krachler, R., Li, Y. & Keppler, B. K. 2011 Preparation and characterization of immobilized [a336][MTBA] in PVA–alginate gel beads as novel solid-phase extractants for an efficient recovery of Hg (II) from aqueous solutions. *Journal of Hazardous Materials* **196**, 201–209. http://dx.doi.org/10.1016/j.jhazmat.2011.09.018.

Zhang, W., Xie, X., Tong, X., Du, Y., Song, Q. & Feng, D. 2021 Study on the effect and mechanism of impurity aluminum on the solvent extraction of rare earth elements (Nd, Pr, La) by p204-p350 in chloride solution. *Minerals* **11** (1), 61. http://dx.doi.org/10.3390/min11010061.

Zheng, H., Li, Y., Zhang, X., Han, J., Li, S., Wu, G., Liu, Q., Liu, X. & Liao, W. 2022 Interaction-determined extraction capacity between rare earth ions and extractants: Taking lanthanum and lutetium as models through theoretical calculations. *Inorganic Chemistry Frontiers* **9** (20), 5360–5370. http://dx.doi.org/10.1039/d2qi01261h.

Zhou, B., Li, Z. & Chen, C. 2017 Global potential of rare earth resources and rare earth demand from clean technologies. *Minerals* **7** (11), 203. http://dx.doi.org/10.3390/min7110203.

First received 31 August 2023; accepted in revised form 11 November 2023. Available online 21 November 2023